J|A|C|S
ARTICLES
Published on Web 01/06/2006

NMR Analysis of Aromatic Interactions in Designed Peptide β-Hairpins

Radhakrishnan Mahalakshmi,[†] Srinivasarao Raghothama,[‡] and Padmanabhan Balaram*,[†]

Contribution from the Molecular Biophysics Unit and NMR Research Center, Indian Institute of Science, Bangalore 560012, India

Received June 17, 2005; E-mail: pb@mbu.iisc.ernet.in

Abstract: Designed octapeptide β-hairpins containing a central ^{D}Pro-Gly segment have been used as a scaffold to place the aromatic residues Tyr and Trp at various positions on the antiparallel β-strands. Using a set of five peptide hairpins, aromatic interactions have been probed across antiparallel β-sheets, in the non-hydrogen bonding position (Ac-L-Y-V-^{D}P-G-L-Y/W-V-OMe: peptides **1** and **2**), diagonally across the strands (Boc-Y/W-L-V-^{D}P-G-W-L-V-OMe: peptides **3** and **6**), and along the strands at positions i and $i + 2$ (Boc-L-L-V-^{D}P-G-Y-L-W-OMe: peptide **4**). Two peptides served as controls (Boc-L-L-V-^{D}P-G-Y-W-V-OMe: peptide **5**; Boc-L-Y-V-^{D}P-G-L-L-V-OMe: peptide **7**) for aromatic interactions. All studies have been carried out using solution NMR methods in $CDCl_3$ + 10% DMSO-d_6 and have been additionally examined in CD_3OH for peptides **1** and **2**. Inter-ring proton−proton nuclear Overhauser effects (NOEs) and upfield shifted aromatic proton resonances have provided firm evidence for specific aromatic interactions. Calculated NMR structures for peptides **1** and **2**, containing aromatic pairs at facing non-hydrogen bonded positions, revealed that T-shaped arrangements of the interacting pairs of rings are favored, with ring current effects leading to extremely upfield chemical shifts and temperature dependences for specific aromatic protons. Anomalous far-UV CD spectra appeared to be a characteristic feature in peptides where the two aromatic residues are spatially proximal. The observation of the close approach of aromatic rings in organic solvents suggests that interactions of an electrostatic nature may be favored. This situation may be compared to the case of aqueous solutions, where clustering of aromatic residues is driven by solvophobic (hydrophobic) forces.

Introduction

Polypeptide chain reversal in proteins is often achieved by the formation of 2-residue turns, commonly referred to as β-turns.[1] β-Hairpins are generated when a centrally positioned β-turn nucleates chain reversal and also facilitates antiparallel registry of the N- and C-terminal strands.[2] The β-hairpin is a structural feature that is widely observed in protein structures and has been the target of several investigations which have focused on design[3] and folding.[4] Model β-hairpins are readily constructed by incorporating a central ^{D}Pro-Xxx segment into designed sequences. This strategy is based on the ability of ^{D}Pro-Xxx to form type II′ β-turns, which fulfill the stereochemical requirements for obtaining a hydrogen bond registry between a pair of antiparallel strands.[5] Analysis of protein crystal structures suggests that hairpin nucleating turns usually prefer the prime stereochemistry.[1] Both type I′ and II′ turns are feasible for Xxx = Gly, while Xxx = L-residues are generally restricted to II′ stereochemistry. Several designed peptide hairpins containing ^{D}Pro-Xxx have been characterized by X-ray diffraction studies,[3b,5c,6] while solution NMR methods have been applied to both hairpins and multistranded β-sheets.[7] The ability to construct well-defined peptide hairpins permits an analysis of side chain interactions, which can, in principle, lend additional stability to this element of secondary structure.

[†] Molecular Biophysics Unit.
[‡] NMR Research Center.

(1) (a) Richardson, J. S.; Richardson, D. C. *Principles and patterns of protein conformation*; Plenum: New York, 1989. (b) Wilmot, C. M.; Thornton, J. M. *J. Mol. Biol.* **1988**, *203*, 221−232. (c) Venkatachalam, C. M. *Biopolymers* **1968**, *6*, 1425−1436.
(2) (a) Gunasekaran, K.; Ramakrishnan, C.; Balaram, P. *Protein Eng.* **1997**, *10*, 1131−1141. (b) Blundell, T. L.; Sibanda, B. L.; Sternberg, M. J.; Thornton, J. M. *Nature* **1987**, *326*, 347−352. (c) Sibanda, B. L.; Thornton, J. M. *Nature* **1985**, *316*, 170−174.
(3) For reviews see: (a) Searle, M. S.; Ciani, B. *Curr. Opin. Struct. Biol.* **2004**, *14*, 458−464. (b) Aravinda, S.; Shamala, N.; Roy, R. S.; Balaram, P. *Proc. Indian Acad. Sci. (Chem. Sci.)* **2003**, *115*, 373−400. (c) Venkatraman, J.; Shankaramma, S. C.; Balaram, P. *Chem. Rev.* **2001**, *101*, 3131−3152. (d) Balaram, P. *J. Pept. Res.* **1999**, *54*, 195−199. (e) Gellman, S. H. *Curr. Opin. Chem. Biol.* **1998**, *2*, 717−725.
(4) (a) Dyer, R. B.; Maness, S. J.; Peterson, E. S.; Franzen, S.; Fesinmeyer, R. M.; Andersen, N. H. *Biochemistry* **2004**, *43*, 11560−11566. (b) Kuznetsov, S. V.; Hilario, J.; Keiderling, T. A.; Ansari, A. *Biochemistry* **2003**, *42*, 4321−4332. (c) Espinosa, J. F.; Syud, F. A.; Gellman, S. H. *Protein Sci.* **2002**, *11*, 1492−1505. (d) Jager, M.; Nguyen, H.; Crane, J. C.; Kelly, J. W.; Gruebele, M. *J. Mol. Biol.* **2001**, *311*, 373−393. (e) Jourdan, M.; Griffiths-Jones, S. R.; Searle, M. S. *Eur. J. Biochem.* **2000**, *267*, 3539−3548. (f) Griffiths-Jones, S. R.; Maynard, A. J.; Searle, M. S. *J. Mol. Biol.* **1999**, *292*, 1051−1069. (g) Munoz, V.; Thompson, P. A.; Hofrichter, J.; Eaton, W. A. *Nature* **1997**, *390*, 196−199.
(5) (a) Haque, T. S.; Gellman, S. H. *J. Am. Chem. Soc.* **1997**, *119*, 2303−2304. (b) Haque, T. S.; Little, J. C.; Gellman, S. H. *J. Am. Chem. Soc.* **1996**, *118*, 6975−6985. (c) Karle, I. L.; Awasthi, S. K.; Balaram, P. *Proc. Natl. Acad. Sci. U.S.A.* **1996**, *93*, 8189−8193. (d) Awasthi, S. K.; Raghothama, S.; Balaram, P. *Biochem. Biophys. Res. Commun.* **1995**, *216*, 375−381.
(6) (a) Harini, V. V.; Aravinda, S.; Rai, R.; Shamala, N.; Balaram, P. *Chem.−Eur. J.* **2005**, *11*, 3609−3620. (b) Aravinda, S.; Harini, V. V.; Shamala, N.; Das, C.; Balaram, P. *Biochemistry* **2004**, *43*, 1832−1846. (c) Aravinda, S.; Shamala, N.; Rajkishore, R.; Gopi, H. N.; Balaram, P. *Angew. Chem., Int. Ed. Engl.* **2002**, *41*, 3863−3865. (d) Karle, I. L.; Das, C.; Balaram, P. *Proc. Natl. Acad. Sci. U.S.A.* **2000**, *97*, 3034−3037.

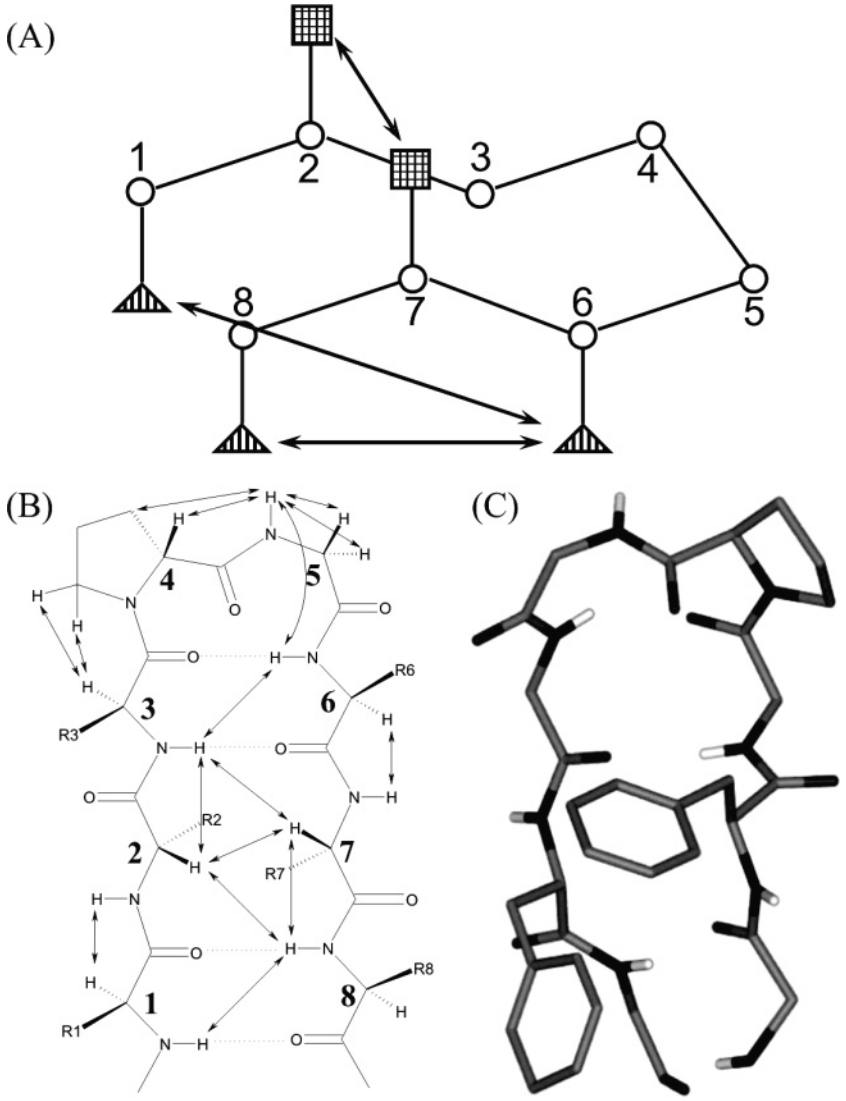

Figure 1. (A) Schematic representation of an octapeptide hairpin showing possible modes of aromatic interactions. The strongest interaction between aromatic residues in synthetic peptide hairpins is anticipated when they are placed at the non-hydrogen bonding position (checked squares) of the strand segments (peptides **1** and **2**). Other modes of interactions include diagonal interactions (peptides **3** and **6**) and interactions along the same strand of the hairpin (peptide **4**), both of which occur when the residues are at the hydrogen bonding position. (B) Schematic representation of an octapeptide hairpin with a nucleating ^{D}Pro-Gly turn. Also marked are the diagnostic β-hairpin NOEs expected in the ROESY spectrum of an octapeptide. (C) An example of a peptide hairpin (-L-F-V-^{D}P-G-L-F-V-OMe segment of a 17-residue peptide) with a type II′ β-turn, showing interacting phenyl rings of Phe residues at the non-hydrogen bonding position.[6d,8o]

β-Hairpins provide an opportunity to investigate tertiary interactions between amino acid side chains which are separated by several residues in the primary sequence. The folded conformation of β-hairpins is principally derived from two stabilizing interactions: hydrogen bonds that are formed between backbone amide groups across the strands and the interactions of side chains that are brought into close proximity. In an antiparallel β-sheet structure, adjacent side chains point on opposite sides of the mean plane of the sheet. The side chains of residues at the i and $i + 2$ positions are therefore spatially proximal. Figure 1A shows a schematic representation of the side chain interactions between nonsequential residues that can occur in a β-hairpin structure. In principle, energetically favorable interactions can occur between side chains at facing non-hydrogen bonding positions and side chains diagonally across antiparallel strands. Several recent studies have focused on introducing aromatic residues in peptide hairpins, to investigate the contribution of aromatic interactions in stabilizing β-hairpin structures and to assess their role in influencing circular dichroism spectra in designed peptides.[8] Earlier analysis of protein crystal structures by Burley and Petsko had suggested that up to 80% of aromatic side chains formed networks that may be important for structure stabilization.[9] Subsequent studies have emphasized the importance of aromatic clusters in lending stability to protein folds.[10] For a pair of proximal phenyl rings, quadrupole−quadrupole interactions have been considered

(7) (a) Langenhan, J. M.; Gellman, S. H. *Org. Lett.* **2004**, *6*, 937−940. (b) Santiveri, C. M.; Rico, M.; Jiminez, A.; Pastor, M. T.; Perez-Paya, E. *J. Pept. Res.* **2003**, *61*, 177−188. (c) Hilario, J.; Kubelka, J.; Syud, F. A.; Gellman, S. H.; Keiderling, T. A. *Biopolymers* **2002**, *67*, 233−236. (d) Venkatraman, J.; Nagana Gowda, G. A.; Balaram, P. *J. Am. Chem. Soc.* **2002**, *124*, 4987−4994. (e) Das, C.; Naganagowda, G. A.; Karle, I. L.; Balaram, P. *Biopolymers* **2001**, *58*, 335−346. (f) Alba, E. D.; Santoro, J.; Rico, M.; Jiminez, A. *Protein Sci.* **1999**, *8*, 854−865. (g) Ramirez-Alvarado, M.; Kortemme, T.; Blanco, F. J.; Serrano, L. *Bioorg. Med. Chem.* **1999**, *7*, 93−103. (h) Stanger, H. E.; Gellman, S. H. *J. Am. Chem. Soc.* **1998**, *120*, 4236−4237. (i) Haque, T. S.; Little, J. C.; Gellman, S. H. *J. Am. Chem. Soc.* **1994**, *116*, 4105−4106.

Table 1. Designed Peptide Hairpins

no.	peptide sequence[a]	mass spectral data (Da)			solvent used for NMR[b]	possible aromatic interactions
		$M + Na^+$	$M + K^+$	M_{calcd}		
1	Ac-L-Y-V-^{D}P-G-L-Y-V-OMe	1000.6	1016.8	978.0	CDDM, CD_3OH	lateral
2	Ac-L-Y-V-^{D}P-G-L-W-V-OMe	1026.1	1041.7	1001.0	CDDM, CD_3OH	lateral
3	Boc-Y-L-V-^{D}P-G-W-L-V-OMe	1081.6	1097.6	1059.0	CDDM	diagonal
4	Boc-L-L-V-^{D}P-G-Y-L-W-OMe	1095.7	1111.8	1073.0	CDDM	alternate
5	Boc-L-L-V-^{D}P-G-Y-W-V-OMe	1084.3	1100.5	1059.0	CDDM	none
6	Boc-W-L-V-^{D}P-G-W-L-V-OMe	1105.9	1122.1	1083.0	CDDM	diagonal
7	Boc-L-Y-V-^{D}P-G-L-L-V-OMe	1009.8	1025.8	986.0	CDDM	none

[a] The one letter code of amino acids is used. ^{D}P = ^{D}Pro; Ac = acetyl; Boc = *tert*-butyloxycarbonyl; OMe = methoxy. [b] CDDM: $CDCl_3$ + 10% DMSO.

dominant.[11] Cross-strand edge-to-face Phe-Phe interactions have been observed from NMR investigations of water-soluble peptide hairpins designed to probe aromatic interactions, suggesting that orientation-dependent stabilizing effects are predominant even in an aqueous environment.[12] These studies suggest an interaction energy of ~ -0.55kcal/mol per Phe-Phe pair. Reports from Cochran's group on "Trp-Trp" pairs in peptide hairpins suggest that aromatic interactions are excellent stabilizing agents of the secondary structure scaffold, which also confer protein-like properties to these peptides.[13] A recent report employing a β-sheet template capable of forming homodimers in organic solvents suggests that "favorable Phe-Phe contacts may not readily occur in the non-hydrogen-bonded cross-strand pairs of antiparallel β-sheets."[14]

In aqueous solutions, strong entropically driven solvent forces such as hydrophobic effects promote clustering of aromatic residues.[15] In contrast, in organic solvents, aromatic interactions must be driven by favorable nonbonded interactions, with weak orientation-dependent electrostatic effects presumably operating as a key stabilizing force. In the present study we report the conformational analysis of seven designed β-hairpin peptides, whose sequences are listed in Table 1. All the peptides examined here are soluble in organic solvents, permitting investigation of aromatic interactions in the absence of solvent driven forces. Sequences of peptides **1**−**6** have been chosen to probe the effects of aromatic pairs involving Tyr and Trp residues at different positions on the β-hairpin (Figure 1A). In all cases, the peptides are protected at the N- and C-termini and are expected to support four intramolecular cross-strand hydrogen bonds in an ideal hairpin conformation (Figure 1B). A view of the molecular conformation in crystals determined for a related hairpin segment containing two facing Phe residues at the non-hydrogen bonding position is illustrated in Figure 1C.[8o] The results described in this paper establish that side chain orientations, which favor close interactions of aromatic rings, are observed for Tyr-Tyr and Tyr-Trp pairs at the non-hydrogen bonding positions of designed β-hairpins even in organic solvents. Aromatic interactions are also observed when the aromatic pairs are placed at the hydrogen bonding positions, but are less pronounced as compared to the non-hydrogen bonding position. Peptides **1** and **2** also provide unusual examples of large upfield shifts for the aromatic proton resonances of Tyr/Trp residues due to ring current effects of a facing aromatic residue.

Experimental Section

Peptide Synthesis: All peptides were synthesized by conventional solution phase chemistry, using a fragment condensation strategy, involving a 3 + 5 coupling in the final step.[16] *tert*-Butyloxycarbonyl (Boc) was used for N-terminal protection, and the C-terminus was protected as a methyl ester. Deprotection of the Boc group was achieved using 98% formic acid, and the methyl ester was removed by saponification using 2N alcoholic NaOH. Peptide couplings were mediated by *N*,*N*′-dicyclohexylcarbodiimide/1-hydroxybenzotriazole (DCC/HOBt). Tyr and Trp residues were used without side chain protection. In peptides **1** and **2**, Ac-Leu was used in the N-terminal fragment. Some of the intermediates were characterized by 80 MHz ^{1}H NMR spectroscopy and thin-layer chromatography (TLC) on silica gel and used without further purification. The final peptides were purified by reverse-phase medium-pressure liquid chromatography (MPLC, C_{18}, 40−60 μ), followed by high performance liquid chromatography (HPLC, C_{18}, 10 μ, 7.8 mm × 250 mm) using methanol−water gradients. The peptides were analyzed by mass spectrometry on a Kompact SEQ MALDI-TOF mass spectrometer (Kratos Analytical, Manchester, UK). Observed and calculated masses are listed in Table 1. All the target peptides were fully characterized by 500 MHz NMR spectroscopy.

NMR: All NMR studies were carried out on a Bruker DRX-500 MHz spectrometer. Selective broadening of the backbone resonances were observed for the peptides in $CDCl_3$ probably due to aggregation of the peptide. Hence, all NMR experiments were carried out in $CDCl_3$ + 10% DMSO-d_6. Peptide aggregation in this case was ruled out by comparing the chemical shifts of backbone resonances in 10mM, 2mM, and 0.4mM peptide in $CDCl_3$ + 10% DMSO-d_6. Complete assignments

(8) (a) Hughes, R. M.; Waters, M. L. *J. Am. Chem. Soc.* **2005**, *127*, 6518−6519. (b) Dhanasekaran, M.; Prakash, O.; Gong, Y. X.; Baures, P. W. *Org. Biomol. Chem.* **2004**, *2*, 2071−2082. (c) Meurisse, R.; Brasseur, R.; Thomas, A. *Proteins: Struct., Funct., Bioinf.* **2004**, *54*, 478−490. (d) Tatko, C. D.; Waters, M. L. *J. Am. Chem. Soc.* **2004**, *126*, 2028−2034. (e) Tatko, C. D.; Waters, M. L. *Org. Lett.* **2004**, *6*, 3969−3972. (f) Waters, M. L. *Biopolymers* **2004**, *76*, 435−445. (g) Butterfield, S. M.; Waters, M. L. *J. Am. Chem. Soc.* **2003**, *125*, 9580−9581. (h) Kiehna, S. E.; Waters, M. L. *Protein Sci.* **2003**, *12*, 2657−2667. (i) Waters, M. L. *Curr. Opin. Chem. Biol.* **2002**, *6*, 736−741. (j) Espinosa, J. F.; Munoz, V.; Gellman, S. H. *J. Mol. Biol.* **2001**, *306*, 397−402. (k) Hunter, C. A.; Lawson, K. R.; Perkins, J.; Urch, C. J. *J. Chem. Soc., Perkin Trans. 2* **2001**, 651−669. (l) Syud, F. A.; Stanger, H. E.; Gellman, S. H. *J. Am. Chem. Soc.* **2001**, *123*, 8667−8677. (m) Espinosa, J. F.; Gellman, S. H. *Angew. Chem., Int. Ed. Engl.* **2000**, *39*, 2330−2333. (n) Santiveri, C. M.; Rico, M.; Jiminez, A. *Protein Sci.* **2000**, *9*, 2151−2160. (o) Zhao, C.; Polavarapu, P. L.; Das, C.; Balaram, P. *J. Am. Chem. Soc.* **2000**, *122*, 8228−8231.
(9) (a) Burley, S. K.; Petsko, G. A. *Adv. Prot. Chem.* **1988**, *39*, 125−189. (b) Burley, S. K.; Petsko, G. A. *Science* **1985**, *229*, 23−28.
(10) (a) Kumar, S.; Nussinov, R. *ChemBioChem* **2002**, *3*, 604−617. (b) Nakamura, H. *Q. Rev. Biophys.* **1996**, *29*, 1−90. (c) Hunter, C. A.; Singh, J.; Thornton, J. M. *J. Mol. Biol.* **1991**, *218*, 837−846.
(11) (a) Chelli, R.; Gervasio, F. L.; Procacci, P.; Schettino, V. *J. Am. Chem. Soc.* **2002**, *124*, 6133−6143. (b) Gervasio, F. L.; Chelli, R.; Procacci, P.; Schettino, V. *Proteins: Struct., Funct., Genet.* **2002**, *48*, 117−125.
(12) Tatko, C. D.; Waters, M. L. *J. Am. Chem. Soc.* **2002**, *124*, 9372−9373.
(13) (a) Cochran, A. G.; Skelton, N. J.; Starovasnik, M. A. *Proc. Natl. Acad. Sci. U.S.A.* **2001**, *98*, 5578−5583. (b) Cochran, A. G.; Tong, R. T.; Starovasnik, M. A.; Park, E. J.; McDowell, R. S.; Theaker, J. E.; Skelton, N. J. *J. Am. Chem. Soc.* **2001**, *123*, 625−632. (c) Russell, S. J.; Cochran, A. G. *J. Am. Chem. Soc.* **2000**, *122*, 12600−12601.
(14) Chung, D. M.; Dou, Y.; Baldi, P.; Nowick, J. S. *J. Am. Chem. Soc.* **2005**, *127*, 9998−9999.
(15) Meyer, E. A.; Castellano, R. K.; Diederich, F. *Angew. Chem., Int. Ed. Engl.* **2003**, *42*, 1210−1250 and references therein.
(16) Awasthi, S. K.; Raghothama, S.; Balaram, P. *J. Chem. Soc., Perkin Trans. 2* **1996**, 2701−2706.

of the resonances were achieved for peptides **1**−**6** using a combination of TOCSY[17] and ROESY[18] experiments. Peptide concentrations of the order of 10 mM were employed for obtaining NMR spectra in $CDCl_3$ + 10% DMSO-d_6 as well as in CD_3OH. All two-dimensional experiments were recorded in phase-sensitive mode using the TPPI method. 1024 and 512 data points were collected in the t2 and t1 dimensions, respectively. NMR data were processed using Bruker XWINNMR software on a Silicon Graphics Indy workstation. The data were zero-filled, and a shifted (π/2) sine square window function was applied to both dimensions, prior to Fourier transformation. Hydrogen bonding information was obtained using chemical shift variations of the amide resonances in the ^{1}H 1D spectrum of individual peptides as a function of temperature.[19] The temperature dependence experiments were carried out in both $CDCl_3$ + DMSO and CD_3OH for peptides **1** and **2** and in $CDCl_3$ + DMSO for peptides **3** to **7**.

Structure Calculations: NOEs were classified as strong, medium, and weak (upper limits for structure calculation were set as 2.5 Å, 3.5 Å, and 5.0 Å, respectively) by visual inspection. Hydrogen bonding information was obtained using temperature-dependent chemical shifts of the amide resonances.[19] Structure calculations were performed using DYANA v1.5.[20] A total of 100 NOEs (60 self, 19 sequential, and 21 long range) were used for peptide **1**. The structures obtained were subsequently refined using 8 angle constraints (ϕ values were used and were obtained from the $^3J_{N\alpha}$ coupling constants) and 4 hydrogen bond constraints. For peptide **2**, 88 NOEs (61 self, 13 sequential, and 14 long range) were employed for structure calculation, and refinement was carried out using 8 angle constraints and 4 hydrogen bond constraints. Structures were refined until there were no violated constraints and short contacts. Of the calculated 30 structures, the best structures were selected and superposed using MOLMOL.[21] Hydrogen-bond distances as well as backbone and side chain torsion angles were calculated for three randomly selected structures and the mean structure and compared.

Circular Dichroism: CD spectra were recorded on a Jasco J-715 CD spectropolarimeter in methanol. Spectra were recorded between 195 nm and 300 nm at 0.1 nm intervals with a time constant of 4 s and a scan speed of 20 nm/min and were averaged over 5 scans. The spectra were baseline corrected and smoothened.

Results and Discussion

All the peptides examined were highly soluble in nonpolar, organic solvents. However, in all cases, broad resonances were obtained for the backbone NH and C$^\alpha$H protons at 500 MHz in chloroform solutions, at the concentrations (10mM) used for NMR experiments. Selective line broadening of backbone proton resonances is indicative of peptide association. This is facilitated by the ready formation of intermolecular hydrogen bonds between structurally well-defined antiparallel strands.[6b] Addition of small amounts of a strongly hydrogen-bonding solvent like DMSO leads to disruption of intermolecular hydrogen-bonded aggregates, resulting in the observation of sharp NH and C$^\alpha$H resonances. Consequently, NMR studies were carried out in a $CDCl_3$−DMSO mixture (10% v/v DMSO in $CDCl_3$)[22] for all the peptides. Peptides **1** and **2** were additionally studied in CD_3OH. Sequence specific assignments for peptides **1**−**6** were achieved using a combination of TOCSY and ROESY experiments (see Supporting Information for tables of chemical shifts, $^3J_{HN-C^\alpha H}$ values and for temperature coefficients of NH chemical shifts). Peptide **7**, which contains a single Tyr residue, served as a control for determining chemical shifts of aromatics protons of the lone Tyr residue, in the absence of aromatic shielding effects.

Backbone Conformations of Peptides 1−6: The backbone conformations of peptides **1**−**6** were inferred from the observed NOEs between backbone NH and C$^\alpha$H protons and the values of the $^3J_{HN-C^\alpha H}$ coupling constants for residues 1−3 and 6−8, which are anticipated to adopt extended strand conformations (see Figure 1B for ideal NOEs expected in octapeptide hairpins). Figures 2A,B and 3A,B illustrate the observed NOEs for peptides **1** and **2**, respectively, in deuterated methanol solutions. The observation of the Tyr2 C$^\alpha$H−Tyr7 C$^\alpha$H NOE together with the presence of the Val3 NH−Leu6 NH and Leu1 NH−Val8 NH NOEs strongly supports a significant population of β-hairpin conformations for peptide **1**. Similarly, the Tyr2 C$^\alpha$H−Trp7 C$^\alpha$H NOE and the Val3 NH−Leu6 NH and Leu1 NH−Val8 NH NOEs are indicative of folded hairpin structures in peptide **2**. Interestingly, in the case of **1**, the Leu1 NH−Tyr2 NH weak NOE is observed, which is suggestive of strand fraying. This NOE is absent in peptide **2**, indicating that the strands in **2** are better ordered than those in **1**. For peptide **1**, a similar pattern of NOEs was also observed in $CDCl_3$−DMSO (see Supporting Information for ROESY spectra of **1** in CD_3OH and $CDCl_3$−DMSO at 300 K). The temperature dependence of NH chemical shifts for peptides **1** and **2** in CD_3OH is summarized in Figures 2C and 3C, respectively. In both cases, large temperature coefficients are observed for the NH protons of residues 2, 5, and 7, which are expected to be solvent exposed in an ideal β-hairpin conformation. The relative insensitivity of the chemical shifts of the NH resonances of residues 1, 3, 6, and 8 is consistent with their involvement in transannular hydrogen bonds.

Figure 4 provides a summary of the key diagnostic hairpin NOEs observed in peptides **3**−**6**, which are compared with the NOEs observed for peptide **1** in $CDCl_3$−DMSO solutions. The Val3 C$^\alpha$H−^{D}Pro4 C$^\delta$H NOE is characteristic of a *trans* Xxx-^{D}Pro bond. This NOE corresponds to a fixed interproton distance of ∼2.1 Å, because the torsion angle ω is fixed to a value of 180°, thus serving as an internal standard for observed NOE intensities. In principle, geminal proton pairs such as the nonequivalent Gly C$^\alpha$H$_2$ or Pro C$^\alpha$H$_2$ protons can also be used as an internal intensity standard. However, because of spectral overlap or small chemical shift differences between the proton pairs in some peptides, we chose to use the Val3 C$^\alpha$H−^{D}Pro4 C$^\delta$H$_2$ NOE as a standard. The remaining four NOEs illustrated in Figure 4 are key diagnostics of an ideal hairpin conformation. It is evident that hairpins are appreciably populated in all cases, although the Leu1 NH−Val/Trp8 NH NOE observed for peptides **5** and **6**, respectively, were weak, suggesting that distortions at the termini may occur in these cases. Fraying of the strands at the N- and C-terminal residues is, however, not uncommon in designed octapeptide hairpins.[6b] Secondary structure information for peptide **7**, derived from $^3J_{HN-C^\alpha H}$ coupling constants, chemical shift dispersion in $CDCl_3$ + 10%

(17) Braunschweiler, L. E.; Ernst, R. R. *J. Magn. Reson.* **1983**, *53*, 521−528.
(18) (a) Bax, A.; Davis, D. G. *J. Magn. Reson.* **1985**, *63*, 207−213. (b) Bothner-By, A. A.; Stephens, R. L.; Lee, J.; Warren, C. D.; Jeanloz, R. W. *J. Am. Chem. Soc.* **1984**, *106*, 811−812.
(19) Raghothama, S.; Chaddha, M.; Balaram, P. *J. Phys. Chem.* **1996**, *100*, 19666−19671.
(20) Guntert, P.; Mumenthaler, C.; Wüthrich, K. *J. Mol. Biol.* **1997**, *273*, 283−298.
(21) Koradi, R.; Billeter, M.; Wüthrich, K. *J. Mol. Graphics* **1996**, *14*, 51−55.
(22) Chemical shifts of the backbone amide and CH resonances were monitored as a function of concentration both in $CDCl_3$ and in $CDCl_3$ + 10% DMSO-d_6. Significant chemical shift variation accompanied by line broadening was observed in $CDCl_3$, while the spectra essentially remained invariant in the latter.

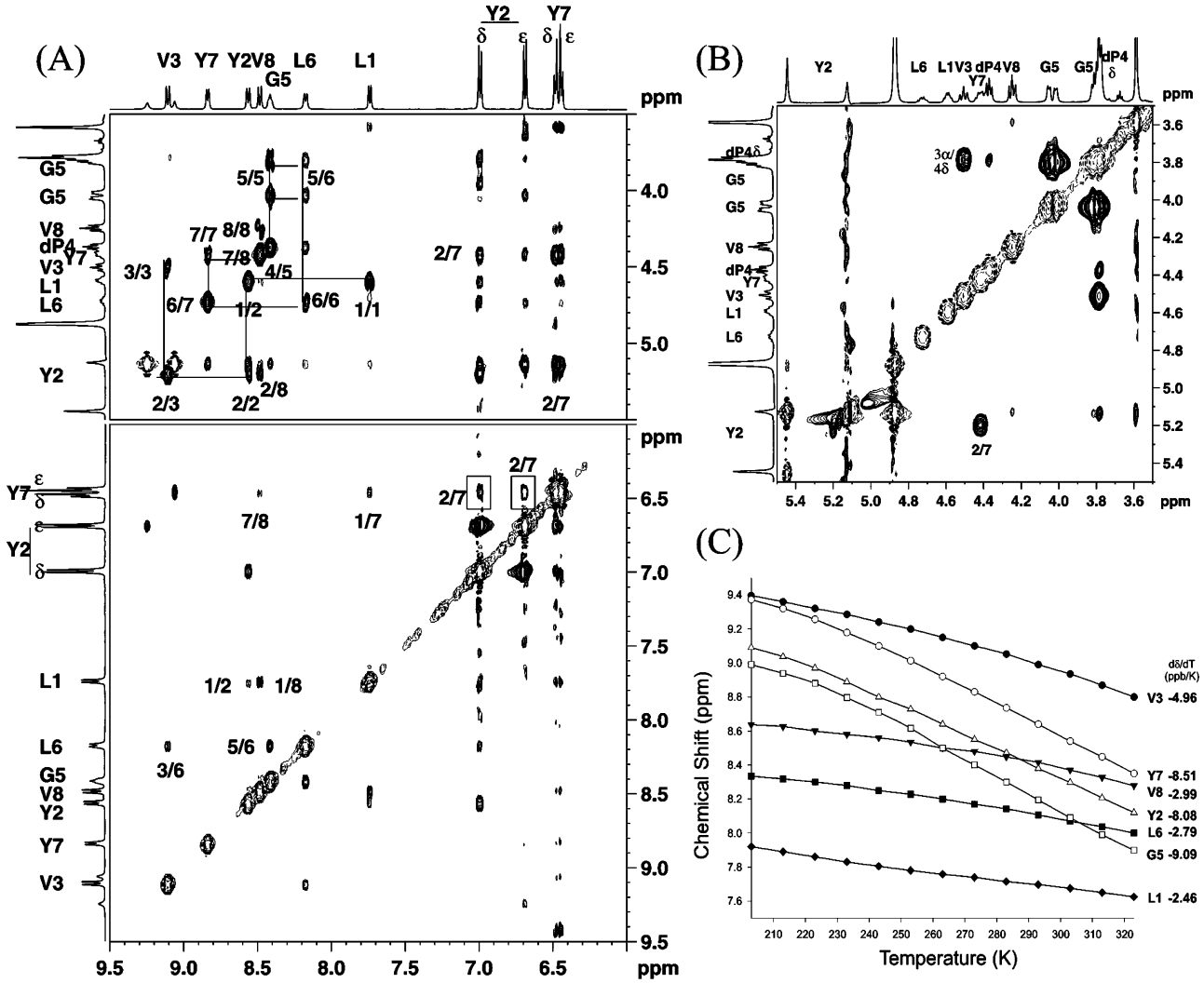

Figure 2. NMR spectra of peptide **1** (Ac-L-Y-V-^{D}P-G-L-Y-V-OMe) in CD_3OH at 273 K. (A) Partial expansions of the ROESY spectrum showing the NH−NH and NH−C$^{\alpha}$H region. (B) ROESY spectrum of **1** showing a strong $d_{\alpha\alpha}$ NOE between Tyr2 and Tyr7. (C) Temperature dependence of the backbone NH resonances to probe exposed vs hydrogen bonded amides.

DMSO and CD_3OH, and the far-UV CD spectrum of the peptide in methanol indicated that the peptide did indeed adopt a well-folded hairpin conformation in both solvent systems. This peptide was specifically designed as a control for obtaining aromatic ring proton chemical shifts in the absence of shielding interactions from other aromatic resonances, and hence further 2D NMR experiments were not carried out.

Aromatic Interactions in Facing Cross-Strand Pairs: In peptide **1**, the aromatic protons of the Tyr2 and Tyr7 residues were clearly separated in both $CDCl_3$−DMSO and CD_3OH solutions. During the course of determining the temperature coefficients of backbone NH chemical shifts in $CDCl_3$−DMSO, we observed that the Tyr7 C$^{\delta}$H and C$^{\epsilon}$H protons showed a significant chemical shift variation with temperature, while the Tyr2 C$^{\delta}$H and C$^{\epsilon}$H were invariant (see Supporting Information). Figure 5A illustrates the temperature dependence of aromatic proton resonances of **1** in methanol. A striking feature of the spectrum at ambient temperature (300 K) is that both sets of Tyr7 aromatic protons appear at significantly higher field than the corresponding Tyr2 protons. The shielding effect is particularly pronounced for the Tyr7 C$^{\delta}$H protons (*meta* to the phenolic hydroxyl). Most dramatically, as the temperature is lowered, the Tyr7 C$^{\delta}$H and C$^{\epsilon}$H resonances become degenerate in chemical shift, resulting in a collapse of the conventional AB spectrum to a single resonance (A_2 spectrum) at 253 K. Aromatic proton assignments were confirmed using natural abundance ^{1}H−^{13}C HSQC spectra, shown in Figure 5B. It should be noted that while ring current effects are expected to strongly influence ^{1}H chemical shifts, the ^{13}C chemical shifts remain largely unaffected.[23] Further cooling results in the extraordinary observation that the Tyr7 C$^{\delta}$H protons appear upfield to the Tyr7 C$^{\epsilon}$H protons (*ortho* to the phenolic hydroxyl group). This unusual shielding effect is undoubtedly a consequence of the orientation of the two facing aromatic rings, with ring current effects contributing very substantially to the observed shielding. Upon heating, downfield shifts of the Tyr7 aromatic protons are observed as a consequence of enhanced populations of alternate rotameric states for the two aromatic rings. Interestingly, a very similar observation of unusual chemical shifts has been reported for Tyr C$^{\delta}$H resonances during an NMR study of a 16-residue fragment, termed "G-peptide" (residues 41−56) from the B1 domain of staphylococcal protein

(23) (a) Iwadate, M.; Asakura, T.; Williamson, M. P. *J. Biomol. NMR* **1999**, *13*, 199−211. (b) Blanchard, L.; Hunter, C. N.; Williamson, M. P. *J. Biomol. NMR* **1997**, *9*, 389−395. (c) Gunther, H.; Schmickler, H.; Konigshofen, H.; Recker, K.; Vogel, E. *Angew. Chem., Int. Ed. Engl.* **1973**, *12*, 243−245.

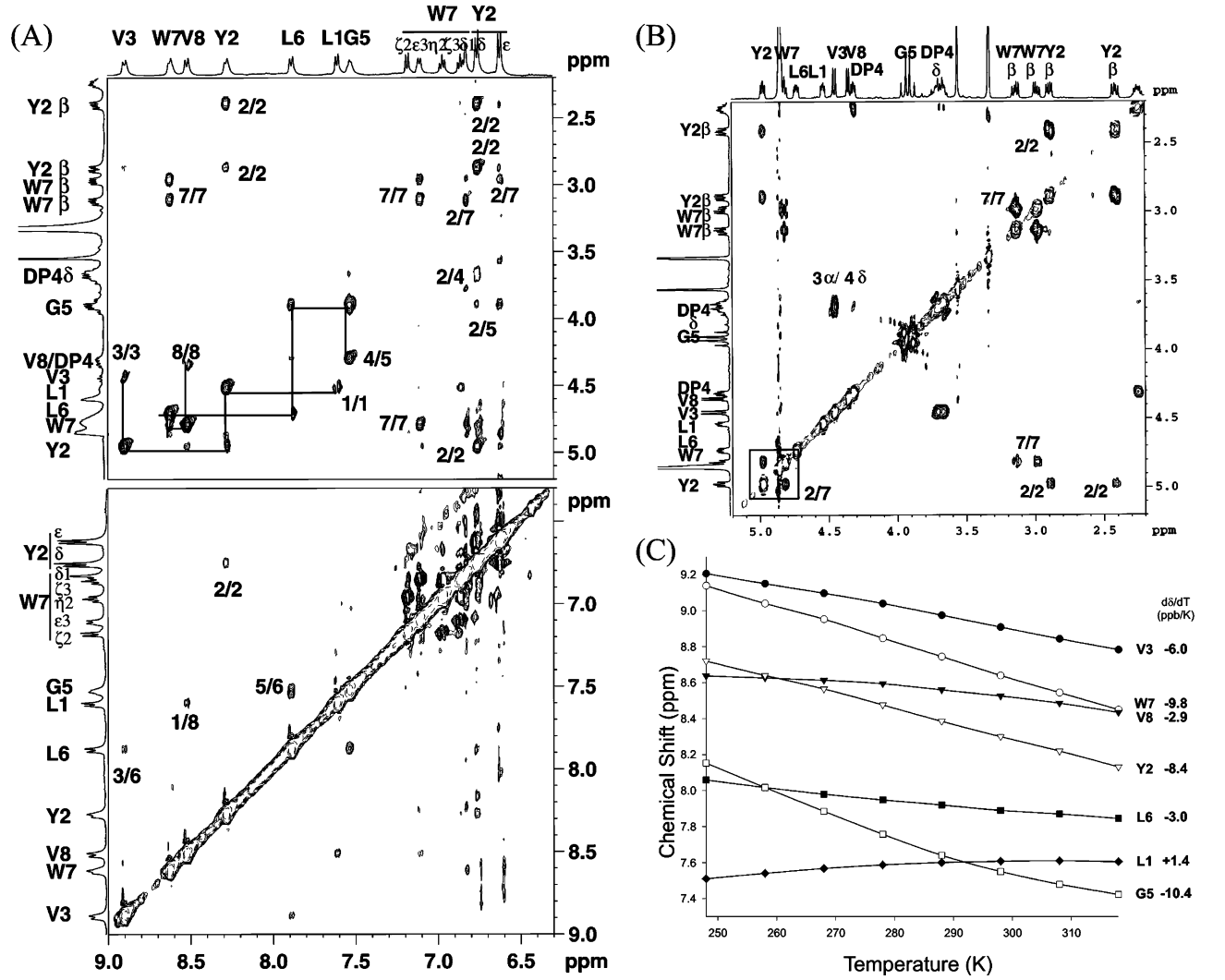

Figure 3. NMR spectra of peptide **2** recorded in methanol at 300 K. (A and B) Partial expansions of the ROESY spectra showing diagnostic hairpin NOEs observed in **2**. (C) Temperature dependence of amide chemical shifts differentiating exposed (open symbols) amides having large temperature coefficients and hydrogen bonded amides (filled symbols) showing small dδ/dT values.

G (Figure 2 of ref 24). In this case, the Tyr ring protons are effectively shielded by the spatially proximal Phe ring. However, the authors did not specifically comment on this spectral feature.

An anomalous temperature dependence of chemical shifts is also observed for the C$^{\epsilon 3}$H proton of Trp7 in peptide **2** (Figure 6) due to shielding effects from the spatially proximal phenolic ring. The C$^{\epsilon 3}$H proton normally appears at ~7.6 ppm for Trp residues.[25] Notably, in **2**, at 298 K, the C$^{\epsilon 3}$H resonance appears at 7.01 ppm, indicative of a very significant upfield shift. At low temperature, ~248−258 K, the estimated chemical shift is ~6.8−6.7 ppm. A curious feature of the low-temperature spectrum, 248−258 K, is the clear doubling of the Trp7 C$^{\zeta 2}$H and C$^{\eta 2}$H proton resonances. The spectral pattern observed for the aromatic multiplets between 6.65 and 6.95 ppm also increases in complexity at low temperature. This is suggestive of slow exchange between alternative orientations of the facing aromatic rings generated by ring flips about the C$^{\beta}$−C$^{\gamma}$ bond as the temperature is lowered. A remarkable high field position for the Trp C$^{\epsilon 3}$H proton (~5.6 ppm) resonance has previously been observed in the 12-residue tryptophan zipper peptide (see Supporting Information of ref 13a).

Proton T1 experiments were performed on both peptides **1** and **2**, to estimate possible differences in the relaxation rates of the phenolic rings when compared to peptide **7**, wherein no intramolecular aromatic interactions are possible (see Supporting Information for T1 values). The T1 values of Tyr ring protons, however, did not vastly differ in the three cases.

The chemical shift index was calculated for peptides **1** and **2** by comparing the observed shifts in methanol relative to random coil shifts for individual residues obtained from the BioMagResBank (BMRB)[26a] and the original report of Wishart, Sykes, and Richards.[26b] This comparison is based on the fact that the intrinsic C$^{\alpha}$H chemical shift in peptides shows little or no solvent dependence. C$^{\alpha}$H resonances of residues 1−3, 6, and 8 showed large downfield shifts, consistent with their presence in β-strand segments (Figure 7). Interestingly, in the case of peptide **1**, the C$^{\alpha}$H resonance of Tyr7 is upfield shifted compared to that of random coil, although 2D NMR experiments establish a

(24) Honda, S.; Kobayashi, N.; Munekata, E. *J. Mol. Biol.* **2000**, *295*, 269−278.
(25) Wüthrich, K. *NMR in biological research: peptides and proteins*; North-Holland Publishing Company: Amsterdam, 1976.
(26) (a) Schwarzinger, S.; Kroon, G. J. A.; Foss, T. R.; Wright, P. E.; Dyson, H. J. *J. Biomol. NMR* **2000**, *18*, 43−48. (b) Wishart, D. S.; Sykes, B. D.; Richards, F. M. *Biochemistry* **1992**, *31*, 1647−1651.

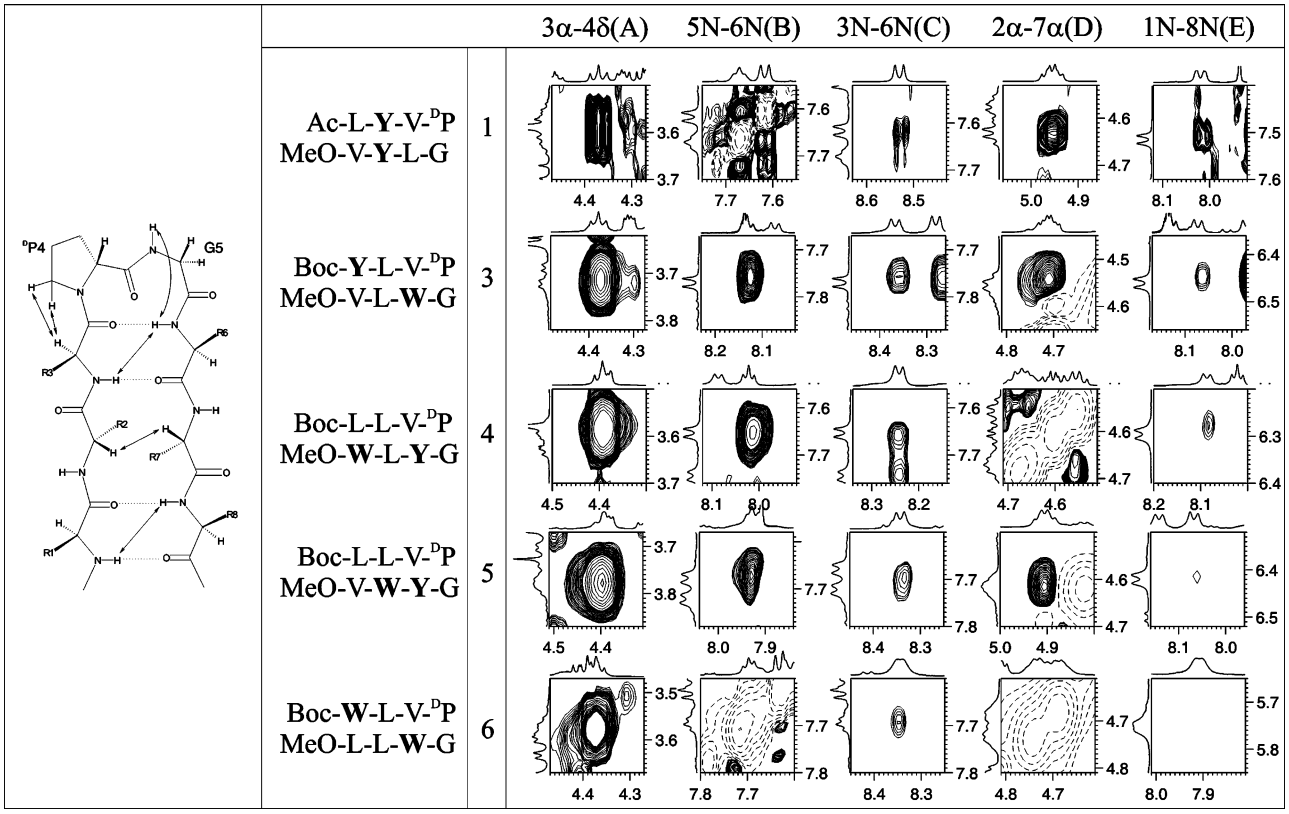

Figure 4. Comparison of intensities of diagnostic hairpin NOEs in peptides **1**, **3**−**6** recorded in $CDCl_3$ + 10% DMSO-d_6 at 300 K. Specific NOEs for the peptides studied are given in each row marked by the peptide number. Columns indicating diagnostic hairpin NOEs are marked as A−E. The 3α-4δ NOE (Column A) intensity was used as a standard. Positive peaks are indicated by solid lines and the diagonal/negative peaks are represented as dashed lines. In the case of 1B and 4D, the cross-peaks are shown on either side of the diagonal. For 6B and 6D, no NOE was observed due to overlapping resonances. In the case of 5E and 6E, very weak NOEs were obtained.

β-hairpin conformation in solution. This anomaly is clearly indicative of the influence of ring currents on the $C^{\alpha}H$ chemical shift. This resonance was also found to be temperature dependent, as established by the $^1H-^{13}C$ HSQC spectra of the peptide recorded at different temperatures (see Supporting Information). Similar effects are anticipated in peptide **2**, wherein the Trp7 $C^{\alpha}H$ proton shows a temperature dependence of chemical shifts. Such anomalous shifts for the $C^{\alpha}H$ resonances due to the influence of a spatially proximal aromatic ring are not uncommon and have been demonstrated in peptide hairpins containing aromatic residues (for examples, see ref 8a, g, and l). Use of chemical shifts to obtain secondary structure information,[26] therefore, is not always applicable in cases of peptides showing strong aromatic interactions, unless the potential ring current effects of nearby aromatic residues are taken into account.

NMR-Derived Structures of Peptides 1 and 2 in CD_3OH: Despite their relatively small size, peptides **1** and **2** yielded a surprisingly large number of interproton NOEs (see Supporting Information), which permitted calculation of solution conformations from the observed NMR data. Figure 8 illustrates the NMR derived structures for the two peptides. Both sequences adopt ideal β-hairpin conformations nucleated by a central ^{D}Pro-Gly type II′ β-turn. The RMSD for the backbone atoms for a family of 15 best NMR structures for **1** is 0.17 ± 0.07 Å and 22 best structures for **2** is 0.06 ± 0.03 Å. The backbone torsion angles for individual structures as well as those averaged over all structures yielded values in very good agreement with those determined for octapeptide hairpins in crystals by X-ray diffraction (Supporting Information; also see backbone torsion angles for peptide hairpins reported in refs 6d and 7e). The observation of several side chain−side chain and side chain−backbone NOEs resulted in a well-defined orientation for the facing aromatic rings in the NMR-derived structures for **1** and **2**. In **1**, both the Tyr rings are oriented over the hairpin backbone with the phenolic rings pointing toward the adjacent C-terminal residues. The phenolic ring centroid to centroid distance between Tyr2 and Tyr7 is 4.66 Å, suggestive of the very close approach of the facing aromatic rings. In protein structures, distances up to 7.0 Å have been considered in identification of interacting aromatic residues.[27] The distances from the centroid of the Tyr2 ring to the C^{δ} and C^{ϵ} protons of Tyr7 are 2.78 Å and 4.19 Å, respectively. The short $C^{\delta}H$ centroid distance is indicative of a strong edge-to-face interaction of the aromatic rings.[12,27] The observed anomalous ring current-induced upfield shift for Tyr7 $C^{\delta}H$ protons is indeed consistent with the NMR-derived structure. Additionally, the short aromatic proton distances obtained for the spatially proximal phenolic rings, in the NMR-

(27) (a) Misura, K. M. S.; Morozov, A. V.; Baker, D. *J. Mol. Biol.* **2004**, *342*, 651−664. (b) Sinnokrot, M. O.; Sherrill, C. D. *J. Am. Chem. Soc.* **2004**, *126*, 7690−7697. (c) Chelli, R.; Gervasio, F. L.; Procacci, P.; Schettino, V. *J. Am. Chem. Soc.* **2002**, *124*, 6133−6143. (d) Gervasio, F. L.; Chelli, R.; Procacci, P.; Schettino, V. *Proteins: Struct., Funct., Genet.* **2002**, *48*, 117−125. (e) Sinnokrot, M. O.; Valeev, E. F.; Sherrill, C. D. *J. Am. Chem. Soc.* **2002**, *124*, 10887−10893. (f) Thomas, A.; Meurisse, R.; Charloteaux, B.; Brasseur, R. *Proteins: Struct., Funct., Genet.* **2002**, *48*, 628−634. (g) Brandl, M.; Weiss, M. S.; Jabs, A.; Suhnel, J.; Hilgenfeld, R. *J. Mol. Biol.* **2001**, *307*, 357−377. (h) McGaughey, G. B.; Gagne, M.; Rappe, A. *J. Biol. Chem.* **1998**, *273*, 15458−15463. (i) Chipot, C.; Jaffe, R.; Maigret, B.; Pearlman, D. A.; Kollman, P. A. *J. Am. Chem. Soc.* **1996**, *118*, 11217−11224. (j) Sun, S.; Bernstein, E. R. *J. Phys. Chem.* **1996**, *100*, 13348−13366. (k) Levitt, M.; Perutz, M. F. *J. Mol. Biol.* **1988**, *201*, 751−754.

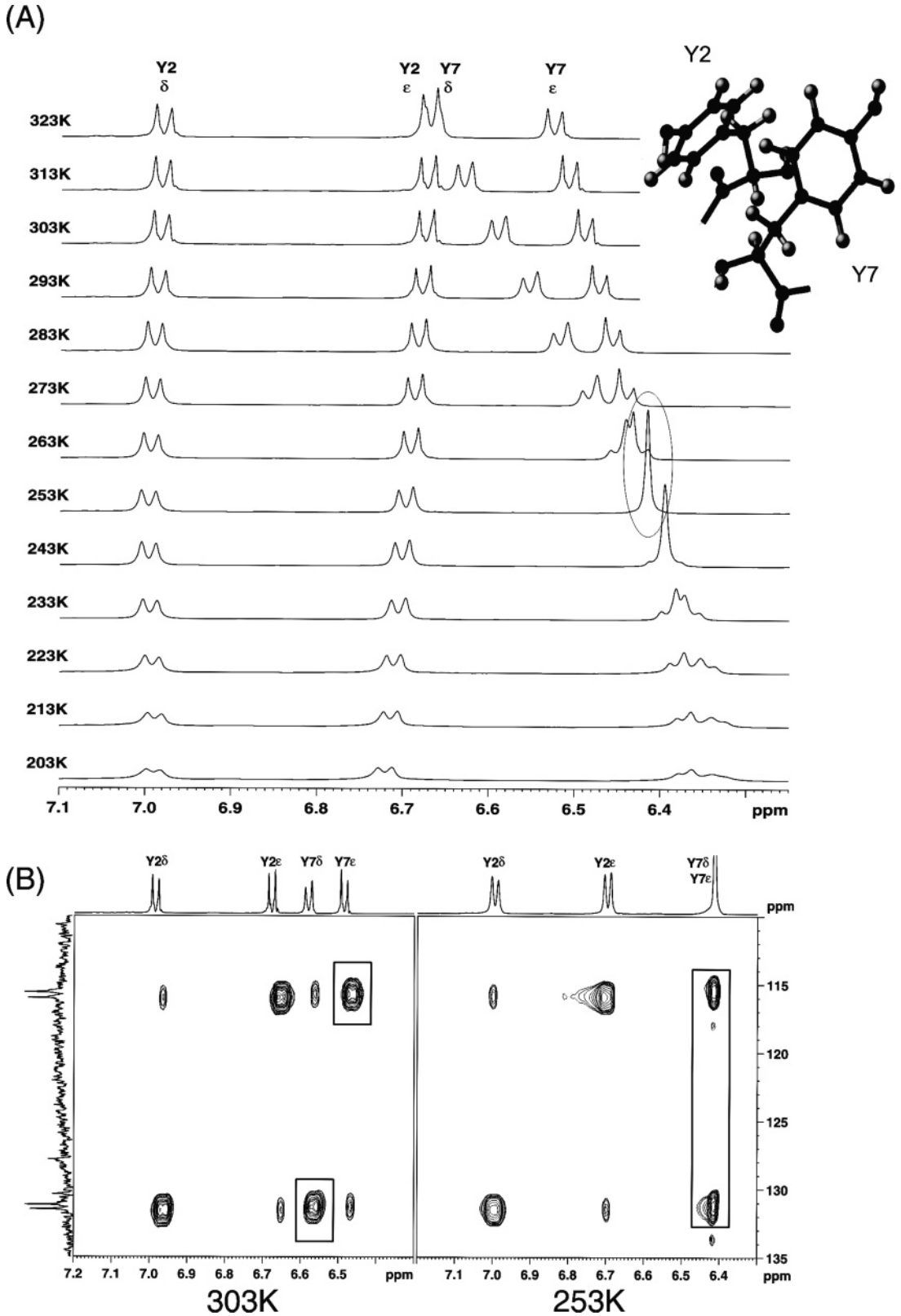

Figure 5. (A) Temperature-dependent chemical shift variation of the aromatic ring proton resonances of Tyr7 in peptide **1**. Inset: ring orientations derived from the solution NMR structure calculated using NOEs obtained in the ROESY spectrum of **1**. Shielding of the Tyr7 ring protons by the spatially proximal Tyr2 ring is evident. (B) Sections of the natural abundance $^{1}H-^{13}C$ HSQC spectrum of **1** in methanol at 303 K (left) compared with the spectrum at 253 K (right). The singlet obtained for Tyr7 phenolic ring in the proton dimension at 253 K can be resolved into two peaks in the ^{13}C dimension.

derived structure, are supported by the strong ring−ring NOEs indicated in Figure 2A.

Ring positions in the structure of peptide **2** were derived from NOEs observed between the indole ring/phenolic ring and the backbone as well as side chains of the residues in the facing strand, as no NOEs were observable between the two aromatic rings. The ring orientations thus deduced correlated well with the observed anomalous chemical shift of the $C^{\epsilon 3}H$ resonance.

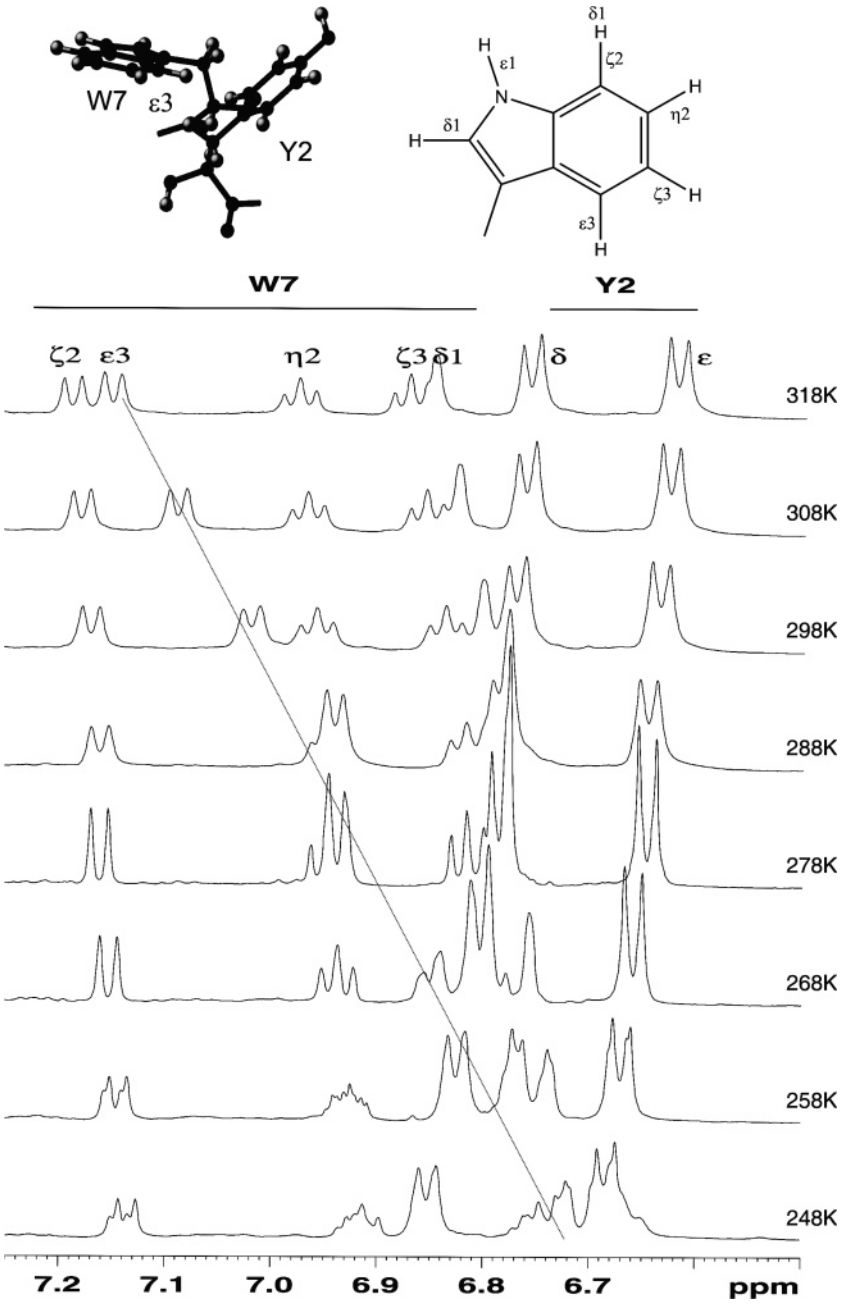

Figure 6. Temperature dependence of aromatic resonances of Trp7 in peptide **2** recorded in methanol. The dotted line highlights the chemical shift variation of the Trp7 $C^{\epsilon 3}H$ resonance.

The orientation of aromatic rings is in a perpendicular fashion and resembles that observed in **1**. The Trp7 $C^{\epsilon 3}H$ group points directly toward the facing Tyr2 ring. The centroid−centroid distances are 6.36 Å and 6.85 Å for the Tyr2-indole six-membered and five-membered rings, respectively. The ring orientation and the observed anomalous chemical shift for the Trp7 $C^{\epsilon 3}H$ resonance correlate well with the results obtained for the Trp-zip peptides,[13a] where strong T-shaped Trp-Trp interactions are observed (see Supporting Information for various ring−ring distances calculated for solution structures of peptide **1** and **2** and a comparison with those derived from the Trp-zip structure 1LE0 (ref 13a)).

Aromatic−Amide Interactions: Interestingly, in both the peptides, the aromatic residues were found to orient themselves toward their respective C-termini. We have previously reported crystal structures of tripeptides containing single aromatic residues and analyzed aromatic−amide pairs in such peptides.[28] It was observed that the aromatic ring almost invariably oriented itself toward the amide plane of the succeeding residue thereby forming strong aromatic−amide interactions. Intramolecular aromatic−amide interactions in small peptides are possible when the side chain torsion angle (χ^1) adopts either a *trans* or *gauche* conformation, assuming that the strands are fully extended ($\phi = -120°$, $\psi = 120°$) and the χ^2 value is about 90° (Distances and angles for an ideal tripeptide segment Ala-Phe-Ala are provided in the Supporting Information). A *trans* conformation favors amide−π interactions with the planar peptide bond of the succeeding residue. A *gauche* conformation results in an aromatic−amide interaction with the preceding residue. However, in the *gauche* conformation, the centroid of the aromatic

(28) Sengupta, A.; Mahalakshmi, R.; Shamala, N.; Balaram, P. *J. Pept. Res.* **2005**, *65*, 113−129.

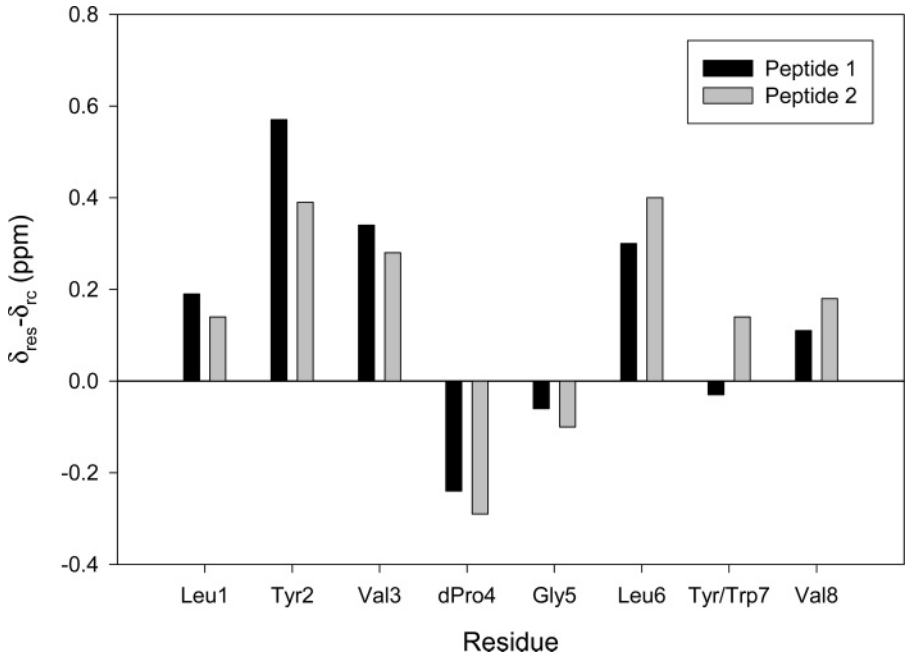

Figure 7. Plot of the variation of $C^{\alpha}H$ chemical shifts with respect to random coil chemical shifts in peptides **1** and **2**. The observed negative value for Tyr7 in peptide **1** is due to shielding effects of the aromatic rings, as deduced from the observed NOEs and large temperature dependence of this resonance.

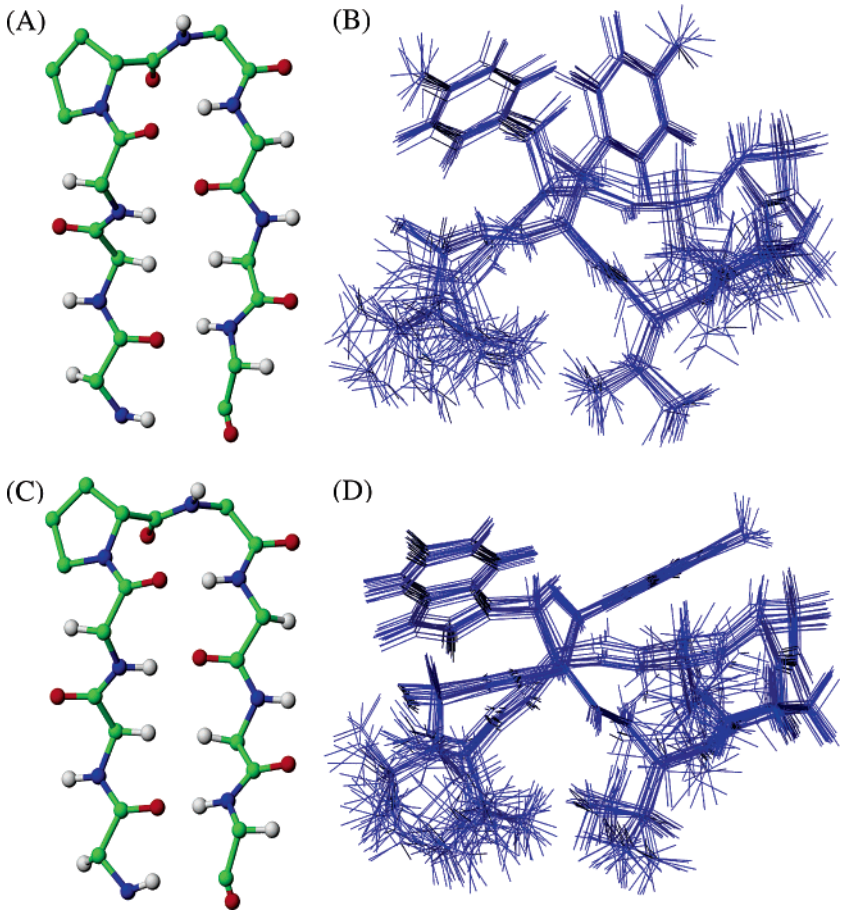

Figure 8. Solution structures of peptides **1** and **2** calculated using DYANA,[20] using NOE information from the ROESY spectra of the individual peptides in methanol. (A and C) Ball-and-stick notation of the backbone atoms in the mean structure of peptides **1** and **2**, respectively. (B) Superposition of 15 best structures calculated for peptide **1**. Mean backbone RMSD: 0.17 ± 0.07 Å. Mean global heavy atom RMSD: 0.90 ± 0.20 Å. (D) Superposition of 22 best structures calculated for peptide **2**. Mean global backbone RMSD: 0.06 ± 0.03 Å. Mean global heavy atom RMSD: 0.78 ± 0.19 Å.

ring lies in close proximity to the carbonyl oxygen of the amide plane. The *trans* conformation brings the centroid above the N−H bond of the peptide unit, an interaction which is evidently more favorable than that obtained in the *gauche* form. Similar ring orientations are seen in the calculated solution structures of peptides **1** and **2** as well as the Trp-zipper peptide[13a] and

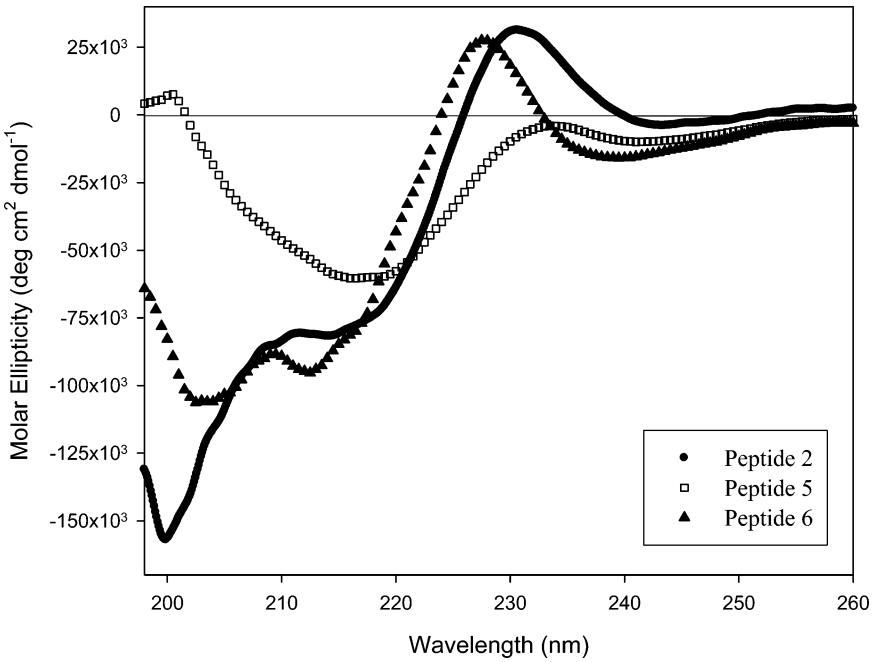

Figure 9. Far-UV circular dichroism spectra of peptides **2** (●), **5** (□), and **6** (▲), recorded in methanol at concentrations of ∼0.5 mg/mL. Shown is the plot of the total molar ellipticity as a function of wavelength.

G-peptide.[24] Analysis of Trp side chain conformations in protein crystal structures, however, reveals an almost equal population of the *trans* and *gauche* conformers,[29] suggesting that other long-range interactions may influence indole ring orientations in proteins.

Aromatic Interactions in Peptides 3−6 in $CDCl_3$ + DMSO-d_6: Most studies of aromatic interactions in proteins have focused on Phe-Phe pairs, for which both the stacked and T-shaped geometries appear to be favorable.[27] In the case of Trp and Tyr residues, the presence of a polar hydrogen bonding group on the aromatic moiety may result in alternate modes of interaction. It was therefore of interest to probe possible aromatic interactions in peptides where Trp and Tyr residues were placed along different positions of the strand segments. Hairpin formation in all four peptides was confirmed by the presence of diagnostic NOEs, as illustrated in Figure 4. It must be noted that, for peptide **6**, two of the four crucial hairpin NOEs were lost due to overlapping resonances. However, information from chemical shift dispersion and $^3J_{HN-C^\alpha H}$ coupling constants enabled us to establish that a substantial population of the peptide adopted the desired β-hairpin conformation. Peptide **5** served as a control for aromatic interactions, as the Tyr and Trp residues in this case were positioned on either face of the mean hairpin plane, preventing intramolecular aromatic interactions in solution when the peptide adopted a β-hairpin conformation.

In the case of peptide **3**, several NOEs between the Y1C$^\delta$H and Y1C$^\epsilon$H resonances to the V8C$^\beta$H and V8C$^\gamma$H protons were seen. In addition, NOEs between the C$^\alpha$H resonances of ^{D}P4 and G5 residues to the C$^\delta$H of W6 indole were also observed. Interestingly, an NOE between Y1C$^\epsilon$H and W6C$^{\eta 2}$H was observed in the ROESY spectrum of the peptide (see Supporting Information), while in peptide **4**, an NOE between the Y6C$^\epsilon$H and W8C$^{\zeta 3}$H protons was detected (see Supporting Information). These ring−ring NOEs are suggestive of aromatic ring proton distances of about ∼3.5 Å, which can be observed for centroid−centroid distances of up to ∼7.0 Å, the reported outer limit for aromatic interactions in proteins.[27] Comparison of the chemical shifts of the aromatic ring protons of peptides **3** and **4** to that of peptide **5**, which serves as a control for aromatic interactions, however showed no drastic differences in the chemical shifts, as was observed in the case of peptides **1** and **2** (see Supporting Information). This observation is not surprising, as effects of ring currents on chemical shifts are dependent on both distance and orientation of one aromatic ring with respect to the other.[30] Peptide **6** had two Trp residues that were expected to be involved in a diagonal aromatic interaction in a well-folded hairpin. We did not however observe any NOEs between the two indole rings in solution. Ring NOEs, if any, were lost due to overlapping aromatic resonances.

Circular Dichroism: Far-UV circular dichroism spectra, which arise due to the n−π* and π−π* transitions of the backbone amide groups, have been widely used for rapid assessment of folded peptide conformations in solution. For β-hairpin peptides, a characteristic broad negative band centered at ∼217 nm has been observed in model hairpins lacking aromatic chromophores.[5d] The presence of aromatic residues can also lead to contributions in the far-UV region, arising from the π−π* transitions of the aromatic rings. Figure 9 shows the far-UV CD spectra of peptides **2**, **5**, and **6**. It is noteworthy that only peptide **5** exhibits a CD spectrum characteristic of a β-hairpin. Both peptides **1** and **2** yielded anomalous far-UV CD spectra, consistent with the observed aromatic interactions in the NMR spectra of these peptides. In the case of peptides **3** and **4**, in addition to the negative band at ∼217 nm, multiple bands which may be ascribed to exciton splitting effect were observed. Interestingly, in peptide **6**, where no inter-ring NOEs

(29) (a) Dunbrack, R. L., Jr. *Curr. Opin. Struct. Biol.* **2002**, *12*, 431−440. (b) Chakrabarti, P.; Pal, D. *Protein Eng.* **1998**, *11*, 631−647.

(30) (a) Emsley, J. W.; Feeney, J.; Sutcliffe, L. *High-resolution nuclear magnetic resonance spectroscopy*; Pergamon: Oxford, 1965; Vol. 1. (b) Johnson, C. E.; Bovey, F. A. *J. Chem. Phys.* **1958**, *29*, 1012−1014.

were obtainable from the NMR spectrum, the far-UV CD spectrum was suggestive of major contributions from aromatic interactions. The anomalous CD spectrum can therefore be ascribed to close proximity of the aromatic rings in the opposing antiparallel strands of the β-hairpin. It should be noted that investigations from the Waters' group has led to the observation that diagonal Trp-Trp pairs in the non-hydrogen bonding position of hairpin scaffolds lead to the formation of a "binding cleft", wherein intercalation of nucleoside moieties can occur.[8g] This immediately suggests that a stacking interaction is likely for Trp residues, when positioned diagonally across the strands. Such π-stacking interactions can equally well be anticipated for peptide **6**, explaining the observed aromatic contributions to the CD spectrum of the peptide. It is therefore quite appropriate to conclude that aromatic contributions, which mask backbone transitions in the far-UV CD spectra,[31] can in fact be used to advantage, for easy and rapid determination of aromatic interactions in peptide scaffolds.

Implications for Aromatic−Aromatic Pairs: The issue currently being debated in the literature is whether interactions between aromatic rings placed at facing positions on antiparallel strands contribute to the stability of β-sheet structures.[8,12−15] While the present study does not directly address the issue of contribution of such interactions to thermodynamic stability, it is noteworthy that the key diagnostic NOEs characteristic of a hairpin fold are most intense in peptides **1** and **2**, which contain strongly interacting aromatic pairs (Figures 2−4). This observation is suggestive of an enhanced population of β-hairpin conformations in these cases. The computation of NOE intensities in Figure 4 provides a rough estimate of the increase in the population of folded conformations in peptides with favorable aromatic interactions. An approximate 2-fold increase in the intensity of diagnostic hairpin NOEs relative to the conformation independent 3α-4δ NOE is observed for peptides **1** and **2**. Quantitation of conformer populations from NOE intensity data cannot be accurately estimated with available data.[32] Dynamic averaging of a heterogeneous population of folded conformations which differ in the number of stabilizing interstrand hydrogen bonds needs to be considered.

An estimate of the stabilizing effects of aromatic interactions on the folded β-hairpin structures may be obtained using backbone chemical shifts of strand residues 2, 3, 6, and 7 (see Supporting Information). Using standard chemical shifts for individual residues in β-sheets obtained from the BMRB database (www.bmrb.wisc.edu) and random coil values from ref 26a, the fraction of folded hairpins may be estimated from observed chemical shift data. The fraction of folded forms in the control peptide Boc-Leu-Val-Val-^{D}Pro-Gly-Leu-Val-Val-OMe[5c,d] is estimated to be 0.28, while, in peptide **1** and **2**, the faction folded is 0.83 and 0.72, respectively. The aromatic contribution to the free energies of stabilization is approximately −0.95 kcal/mol and −0.57 kcal/mol for peptides **1** and **2**, respectively. These numbers are in good agreement with estimates for aromatic interactions in other systems.[8d]

(31) In the presence of aromatic contributions, secondary structure analysis using far-UV CD spectra is not possible.[8o] In such cases, vibrational circular dichroism (VCD) provides an attractive alternative (Mahalakshmi, R.; Shanmugam, G.; Polavarapu, P. L.; Balaram, P. *ChemBioChem* **2005**, *6* 2152−2158).

(32) Blackledge, M. J.; Bruschweiler, R.; Griesinger, C.; Schmidt, J. M.; Xu, P.; Ernst, R. R. *Biochemistry* **1993**, *32*, 10960−10974.

Table 2. Side Chain Torsion Angles Obtained for Representative Peptide and Protein Hairpins Showing Edge-to-Face Aromatic Interaction

residue	χ^{1}[a,b]	χ^{2}[a]
Ac-Leu-Tyr-Val-^{D}Pro-Gly-Leu-Tyr-Val-OMe (NMR) (this study)		
Tyr2	−49.0 (*g*)	129.2
Tyr7	162.1 (*t*)	109.9
Ac-Leu-Tyr-Val-^{D}Pro-Gly-Leu-Trp-Val-OMe (NMR) (this study)		
Tyr2	−71.1(*g*)	122.2
Trp7	176.8 (*t*)	−81.8
Boc-Leu-Phe-Val-Aib-^{D}Ala-Leu-Phe-Val-OMe (X-ray)[6c]		
Phe2	−67.3(*g*)	−106.8
Phe7	−174.1 (*t*)	−104.1
- -Leu-Phe(11)-Val-^{D}Pro-Gly-Leu-Phe(16)-Val-OMe (X-ray)[6d]		
Phe11	−69.0 (*g*)	−86.0
Phe16	−172.0 (*t*)	−99.0
H_2N−SW(2)TW(4)EGNKW(9)TW(11)K−$CONH_2$(1LE0) (NMR)[13a]		
Trp2	−63.9 (*g*)	117.8
Trp4	174.6 (*t*)	−104.4
Trp9	−64.2 (*g*)	100.2
Trp11	−170.4 (*t*)	−100.6
- -EWTY(45)DDATKTF(52)TVTE-COOH (1PGA) (X-ray)[24]		
Tyr45	168.0 (*t*)	−113.6
Phe52	−75.9 (*g*)	−102.2
- -LW(153)CNGRW(158)V- - (1BGL) (X-ray)[36]		
Trp153	−70.7 (*g*)	−110.4
Trp158	−173.4 (*t*)	80.7
- -LY(150)NNGTY(155)M- - (1QHO) (X-ray)[37]		
Tyr150	−64.0 (*g*)	−105.2
Tyr155	−176.3 (*t*)	69.1
- -TY(191)QNGYY(196)Y- - (1UV4) (X-ray)[38]		
Tyr191	179.7 (*t*)	−104.3
Tyr196	−64.9 (*g*)	−82.0
- -KY(102)VNGEW(107)V- - (1XBR) (X-ray)[39]		
Tyr102	−154.0 (*t*)	−113.8
Trp107	−81.8 (*g*)	107.6

[a] Torsion angle χ^{n} for the side chain follows the convention presented in IUPAC-IUB Commission on Biochemical Nomenclature *Biochemistry*, **1970**, *9*, 3471−3479. [b] In the edge-to-face pair, the ring which served as the "face" for aromatic interaction was seen to prefer the *gauche* (*g*) conformation, whereas the other interacting ring was seen to adopt a *trans* (*t*) conformation.

Several reports using model water-soluble hairpins argue that facing aromatic pairs contribute significantly to structure stabilization.[8b,d,f,h,13a] The work of Tatko and Waters also emphasizes the fact that specific edge-to-face interaction geometries arise due to electronic and/or van der Waals interactions and are not driven exclusively by the hydrophobic effect.[12] Our studies, in organic solvents, permit a separation between the role of solvent entropy and favorable enthalpic interactions in determining the orientations of proximal aromatic rings in antiparallel β-sheets. The observation of a T-shaped geometry for facing aromatic residues Tyr/Trp in peptides **1** and **2** in weakly solvating media like $CDCl_3$ and CD_3OH suggests that such a disposition of aromatic rings is indeed energetically favorable. In principle, aromatic side chains can adopt different orientations corresponding to specific values of the torsion angles χ^{1} and χ^{2}. The aromatic ring adopts completely different orientations with respect to the peptide backbone in the three possible rotamers about the $C^{\alpha}-C^{\beta}$ bond (χ^{1}). For the edge-to-face interactions to occur, χ^{1} must adopt the *trans* conformation at one residue and the *gauche* conformation at the other aromatic amino acid of the interacting pair (Table 2). Other rotameric possibilities, which are also locally favorable, do not lead to spatial proximity between the two rings or can

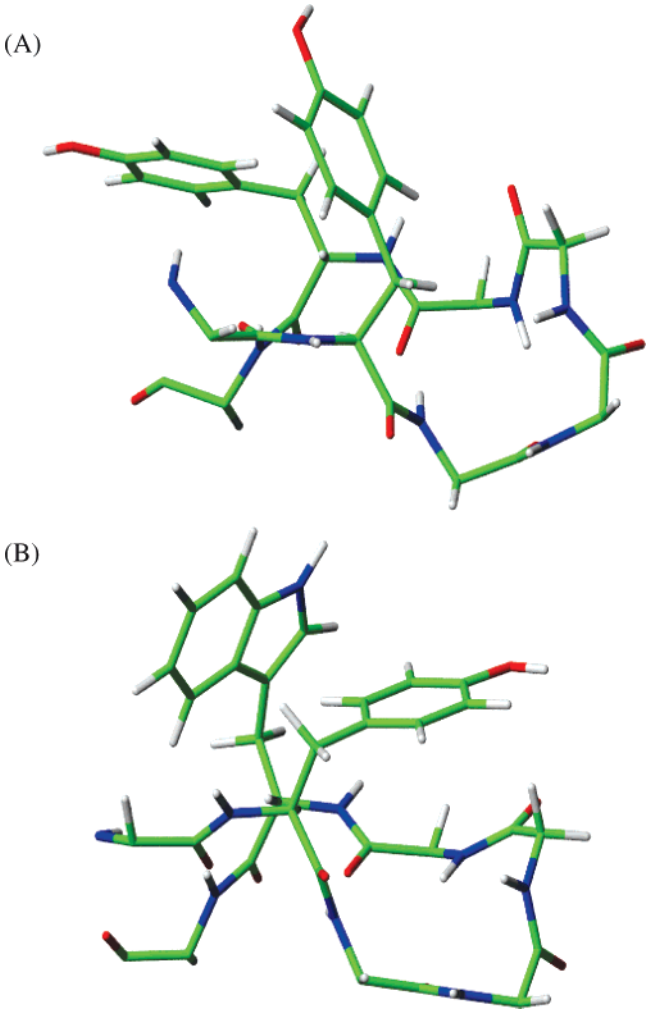

Figure 10. Representative examples of T-shaped aromatic interactions found at the non-hydrogen bonding position of hairpins in proteins. (A) 1QHO[37] showing edge-to-face Tyr-Tyr interaction. (B) 1XBR[39] with T-shaped Tyr-Trp interaction.

result in unfavorable steric contact (Figure S28 in Supporting Information lists the inter-ring distances for different combination of side chain torsion angles). The observation of a specific inter-ring geometry in organic solvents argues strongly that the observed orientations are energetically favorable. A preliminary analysis of available protein structures from the Protein Data Bank (PDB)[33] revealed that T-shaped aromatic interactions are also found at the non-hydrogen bonding position of hairpin structures in proteins. Two such examples are illustrated in Figure 10. The side chain torsion angles obtained for such aromatic interactions in proteins correlated well with those observed in peptides (Table 2).

Interestingly, in crystal structures of the protected tripeptides containing the L−W/F−V segment, in which the peptide backbone adopts an extended β-sheet conformation, the aromatic rings adopt other rotameric states, suggesting that the observed choice in the hairpin scaffold may be driven by favorable interactions.[28] These observations are at variance with the recent suggestion by the group of Nowick[14] that favorable aromatic interactions do not play a significant role in β-sheet stabilization.

(33) Berman, H. M.; Westbrook, J.; Feng, Z.; Gilliland, G.; Bhat, T. N.; Weissig, H.; Shindyalov, I. N.; Bourne, P. E. *Nucleic Acids Res.* **2000**, *28*, 235−242.

In the model system chosen, potential Phe-Phe interactions across an antiparallel β-sheet dimer interface have been probed by replacing Phe residues by the hydrogenated analogue cyclohexylalanine (Cha). Notably, a central Phe-Phe interaction has been retained in all the systems studied. As noted by Nowick and co-workers, the twist angle between antiparallel β-strands may also influence aromatic interactions. The extent of twist is likely to be different in intramolecular hairpins as compared to model systems in which flatter sheets are likely to be formed by peptide association.[34] In hairpins, the extent of twist can be determined by the nature of the nucleating β-turn with the type I′ turn generating a significantly higher degree of twist.[6c] Comparison of peptide crystal structures nucleated by a type I′ turn[6c] with those nucleated by II′ turns[6d] suggests that aromatic interactions at facing non-hydrogen bonded sites are indeed possible in these cases.

Conclusions

Protein folding is driven by noncovalent interactions such as hydrogen bonding, salt bridges, and dipole−dipole and hydrophobic interactions.[35] Of these forces, the initial folding process is believed to be driven by a "hydrophobic collapse" wherein the apolar and aromatic residues tend to associate with each other, excluding solvent molecules, giving rise to the molten globule.[35] In the equation for the free energy of folding $\Delta G = \Delta H - T\Delta S$, increased solvent entropy following the hydrophobic collapse contributes significantly to the entropic (ΔS) term, thereby lowering ΔG, driving folding. In organic solvents, however, association of apolar residues is not necessarily solvent driven. Under these conditions, the contribution of entropically driven solvent forces to the free energy of folding is minimal. Secondary structure formation and folding in organic solvents is driven primarily by enthalpy, with predominant contributions from intramolecular hydrogen bonding, van der Waals forces, dipole−dipole, and quadrupole interactions.[9] Model peptides soluble in organic solvents are good examples for investigating the enthalpic contribution toward folding and stability. Additionally, such peptides form good models for studying the hydrophobic protein interior and the preferred modes of association and packing of specific aromatic residues.

In the present study, we have analyzed aromatic interactions between Trp and Tyr residues incorporated in predefined β-hairpin scaffolds. The high solubility of these peptides in organic solvents permits the investigation of possible modes of "aromatic interaction" in the absence of solvent-driven hydrophobic forces. Our results show clear evidence for strong T-shaped interactions between the side chains of aromatic

(34) (a) Yang, A. S.; Honig, B. *J. Mol. Biol.* **1995**, *252*, 366−376. (b) Murzin, A. G.; Lesk, A. M.; Chothia, C. *J. Mol. Biol.* **1994**, *236*, 1382−1400. (c) Nishikawa, K. S.; Chou, K. C.; Nemethy, G.; Scheraga, H. A. *J. Mol. Biol.* **1983**, *168*, 389−407. (d) Salemme, F. R.; Weatherford, D. W. *J. Mol. Biol.* **1981**, *146*, 119−141. (e) Scheraga, H. A. *Macromolecules* **1976**, *9*, 395−407. (f) Chothia, C. *J. Mol. Biol.* **1973**, *75*, 295−302.

(35) Voet, D.; Voet, J. G. *Biochemistry*, 2nd ed.; Wiley: New York, 1995. Creighton, T. E. *Proteins: Structures and molecular properties*, 2nd ed.; Freeman: New York, 1993. Branden, C.; Tooze, J. *Introduction to Protein Structure*, 2nd ed.; Garland: New York, 1999.

(36) Jacobson, R. H.; Zhang, X.; Dubose, R. F.; Matthews, B. W. *Nature* **1994**, *369*, 761−766.

(37) Dauter, Z.; Dauter, M.; Brzozowski, A. M.; Christensen, S.; Borchert, T. V.; Beier, L.; Wilson, K. S.; Davies, G. J. *Biochemistry* **1999**, *38*, 8385−8392.

(38) Proctor, M.; Taylor, E.; Nurizzo, D.; Turkenburg, J.; Lloyd, R.; Vardakou, M.; Davies, G.; Gilbert, H. *Proc. Natl. Acad. Sci. U.S.A.* **2005**, *102*, 2697−2702.

(39) Muller, C. W.; Herrmann, B. G. *Nature* **1997**, *389*, 884−888.

residues, when they are placed at the non-hydrogen bonding position of preformed hairpin scaffolds. Additionally, we have also obtained upfield chemical shifts for ring proton resonances due to shielding effects of a spatially proximal aromatic ring. These observations clearly indicate the presence of a large population of well-folded hairpins stabilized by tertiary interactions, even in apolar solvents. Our results therefore suggest a preference for the edge-to-face mode of aromatic interaction, despite several available combinations of allowed side chain torsion angles at the non-hydrogen bonding position of the peptide hairpin. This observation is supported by several reports in the literature as well as examples from the PDB.[8b,d,o,12,13a] Additionally, the peptides adopt a significant twist along the backbone, as is seen in β-sheet structures of proteins. In the case of peptides with aromatic residues at the hydrogen bonding position, namely, diagonal interactions across facing strands as well as interactions along the same face of the strand, distinct NOEs were obtained. These results suggest that, even in organic solvents, cross-strand aromatic interactions do exist, probably driven by quadrupole interactions. The results presented in this report may be of interest in the de novo design of stable secondary structure scaffolds in which backbone dynamics is restricted by the incorporation of specifically designed tertiary interactions involving aromatic residues.

Acknowledgment. R.M. is supported by the award of a Senior Research Fellowship from the Council of Scientific and Industrial Research (CSIR), India. This work is supported by a program in the area of Molecular Diversity and Design funded by the Department of Biotechnology, Government of India.

Supporting Information Available: NMR data for all peptides. This material is available free of charge via the Internet at http://pubs.acs.org.

JA054040K